

# Planar capacitive sensors – designs and applications

*Xiaohui Hu and Wuqiang Yang*

School of Electrical and Electronic Engineering, The University of Manchester, Manchester, UK

### Abstract

**Purpose** – The purpose of this paper is to present the sensing mechanism, design issues, performance evaluation and applications for planar capacitive sensors. In the context of characterisation and imaging of a dielectric material under test (MUT), a systematic study of sensor modelling, features and design issues is needed. In addition, the influencing factors on sensitivity distribution, and the effect of conductivity on sensor performance need to be further studied for planar capacitive sensors.

**Design/methodology/approach** – While analytical methods can provide accurate solutions to sensors of simple geometries, numerical modelling is preferred to obtain sensor response to different design parameters and properties of MUT, and to derive the sensitivity distributions of various electrode designs. Several important parameters have been used to evaluate the response of the sensors in different sensing modes. The designs of different planar capacitive sensor arrays are presented and experimentally evaluated.

**Findings** – The response features and design guidelines for planar capacitive sensors in different sensing modes have been summarised, showing that the sensor in the transmission mode or the single-electrode mode is suitable for material characterisation and imaging, while the sensor in the shunt mode is suitable for proximity/displacement measurement. The sensitivity distribution of the sensor depends largely on the geometry of the electrodes. Conductivity causes positive changes for the sensor in the transmission and single-electrode mode, but negative changes for the sensor in the shunt mode. Experimental results confirm that sensing depths of the sensor arrays and the influence of buried conductor on capacitance measurements are in agreement with simulations.

**Research limitations/implications** – Experimental verification is needed when a sensor is designed.

**Originality/value** – This paper provides a comprehensive study for planar capacitive sensors in terms of sensor design, evaluation and applications.

**Keywords** Sensors, Design, Modelling, Physical properties of materials, Image sensors

**Paper type** Research paper

### Introduction

Capacitive sensors have been used for a wide range of applications due to their features: low cost, fast response, non-intrusive and non-invasive, no radiation and flexibility in electrode design (Huang *et al.*, 1989; Xie *et al.*, 1990). In a planar capacitive sensor, the sensor electrodes are placed in a co-planar plane. Apart from the above common features, the planar structure provides a possibility to interrogate a material under test (MUT) from only one side (Mamishv *et al.*, 2004), which is particularly useful when the access to an MUT is limited. These additional features make planar capacitive sensors a popular option for applications in proximity/displacement measurement (Chen and Luo, 1998), intelligent human interfacing (Smith *et al.*, 1998), non-destructive testing (NDT) (Diamond and Hutchins, 2006), material characterisation (Mamishv *et al.*, 2004) and imaging

(Frounchi and Dehkhoda, 2003; Cheng, 2008). On the other hand, the planar structure complicates sensor design, especially with different properties of MUT and conditions.

Some work has been done in sensor design and evaluation of planar capacitive sensors. A rectangular-shaped sensor array (Shi *et al.*, 1991) and a comb-shaped sensor array (Wang *et al.*, 1996) were studied for multi-interface detection between air/oil/water, showing that an optimal set of structural parameters can be used to achieve the desired sensitivity and linearity. For NDT and material characterisation, Igreja and Dias (2004) studied the design issues for an inter-digital sensor using an analytical method. Li *et al.* (2006) used a numerical method to study a concentric ring sensor, with an emphasis on the effects of shielding and substrate thickness. General design principles have been given by Igreja and Li for the respective sensors. For proximity or displacement measurement-related applications, the existing studies mainly focus on conductive MUT. For example, Chen and Luo (1998) used an analytical method to study the performance of a concentric-ring-shaped sensor for proximity measurement of a grounded metal disk, where the influence of electrode size, shape and geometry was considered. Using a

---

The current issue and full text archive of this journal is available at [www.emeraldinsight.com/0260-2288.htm](http://www.emeraldinsight.com/0260-2288.htm)



Sensor Review  
30/1 (2010) 24–39  
© Emerald Group Publishing Limited [ISSN 0260-2288]  
[DOI 10.1108/02602281011010772]

---

Drs Min Yang and Bin Cheng are thanked for their useful discussions and contributions to this work.

numerical method, Zeothout *et al.* (2003) studied a rectangular shaped planar sensor for displacement measurement of a grounded spindle, and also compared the performance of the sensor with different material properties and boundary conditions. With a single-electrode array, Lee *et al.* (1999) studied the performance of a capacitive fingerprint sensor, where the sensor output against the distance between the fingers and the sensing chip was studied.

In the context of characterisation and imaging of a dielectric MUT with different boundary conditions, however, a systematic study of sensor modelling, features and design issues is needed. In addition, the influencing factors on sensitivity distribution, and the effect of conductivity on sensor performance need to be further studied for planar capacitive sensors.

This paper discusses planar capacitive sensors in terms of their sensing mechanism, reviews key issues in design and evaluation, with a focus on characterisation and imaging of dielectric MUTs. Further investigations of the sensor responses under different conditions have been carried out using a numerical method. The applications of planar capacitive sensors are summarised according to sensor features and different methods for image reconstruction, and an application example is given to illustrate the design and evaluation of planar capacitive sensors.

## Capacitive sensing

### Sensing principle

The principle of capacitive sensing is based on the interaction between an MUT and the interrogating electric field. An electric field generated from sensor electrodes penetrates through an MUT, and causes electric displacement within the MUT to counter the applied field. This displacement field changes the charge stored between the sensor electrodes, and thus alters inter-electrode capacitance, which in turn can be used to infer the properties of the MUT, such as permittivity, conductivity and their distributions, and ultimately to derive the system variables, such as moisture, temperature, that can be related to those properties.

For capacitance measurement, an electrical stimulus is applied to a driving electrode while a measurement is taken from a sensing electrode. Usually, the frequency of the electrical stimulus, and thus the generated electric field, is limited. For example, the frequency range of the state-of-the-art Agilent precision impedance analyser 4294A is between 40 and 110 MHz (Agilent, 2008b). In this frequency range, an MUT can be mainly characterised by its static relative permittivity and conductivity (Da Silva, 2008). The interaction between an MUT and electric field can be described by the Laplace equation for electro-static or electro-quasi-static approximation, assuming no free charge in the sensing space (COMSOL, 2008):

$$\nabla \left( \frac{\sigma(\mathbf{r}) + \varepsilon_0 \varepsilon(\mathbf{r})}{T} \right) \nabla \Phi(\mathbf{r}) = 0 \quad (1)$$

$$\nabla \left( \frac{\sigma(\mathbf{r}) + j\omega \varepsilon_0 \varepsilon(\mathbf{r})}{T} \right) \nabla \Phi(\mathbf{r}) = 0 \quad (2)$$

where:

- $\mathbf{r}$  position vector.
- $\sigma(\mathbf{r})$  spatial conductivity distribution.
- $\varepsilon_0$  permittivity of vacuum.

- $\varepsilon(\mathbf{r})$  spatial relative permittivity distribution.
- $\Phi(\mathbf{r})$  spatial electric potential distribution.
- $\nabla$  gradient operator.
- $T$  time constant for electro-static approximation.
- $\omega$  angular frequency of the electric field.

In equation (1), the electro-statics formulation is approximated for conducting and dielectric materials. In equation (2), the electro-quasi-statics formulation is approximated for conducting and dielectric materials with small currents and a negligible coupling between the electric and magnetic fields.

When electric potentials are applied to a sensing system, including the sensor electrodes and an MUT, a specific set of boundary conditions is defined. By solving the field equations with the imposed potential boundary conditions, the relationship between capacitance of any pair of electrodes and the distributions of permittivity and conductivity in the system can be derived by Yang and Peng (2003):

$$C = \frac{Q}{V} = -\frac{1}{V} \oint (\sigma(\mathbf{r}) + \varepsilon_0 \varepsilon(\mathbf{r})) \nabla \Phi(\mathbf{r}) d\Gamma \quad (3)$$

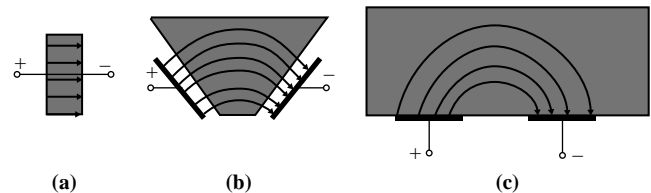
where:

- $V$  electric potential difference between a pair of electrodes.
- $\Gamma$  electrode surface.

### Planar sensor structure and different sensing modes

Conventionally, a capacitor is in the form of a parallel-plate, where the driving and sensing electrodes are placed opposite to each other in close proximity. An electric field is uniformly distributed between them. When the electrodes gradually open up, the electric field is no longer confined within a small region between the electrodes, but expanded into a wider space and forms a fringe field. When the electrodes are open up to a co-planar plane, the fringe field becomes predominant between the driving and sensing electrodes. This type of sensor is called planar sensor in literature. The transition from a parallel-plate capacitor to a planar sensor with the consideration of the fringe effect is shown in Figure 1 (Mamishv *et al.*, 2004). The planar structure provides a possibility to interrogate an MUT from only one side (Mamishv *et al.*, 2004), which is particularly useful when the access to both sides of an MUT is limited. For example, to inspect the surface or the internal properties of a large mechanical structure, the sensor electrodes can only scan over its surface to acquire information. To scan a foot with a shoe on, the electrodes can only be placed on the bottom of the shoe. The associated design issues for planar sensors are more complicated than the conventional capacitance sensors.

**Figure 1** Transition from parallel-plate to fringe field sensor



**Notes:** (a) Parallel-plate capacitor whose; (b) electrodes open up to provide; (c) one-sided access to MUT

From equation (3), the value of the inter-electrode capacitance depends on the geometries of the sensor and the MUT, the distributions of permittivity and conductivity in the system, and the potential boundary conditions. This means that an inter-electrode capacitance can change with an MUT being dielectric or conductive, floating or grounded. When an MUT is surrounded by sensor electrodes, the system boundary conditions are specified by the status of the sensor electrodes. For a planar capacitance sensor, however, the potential boundary conditions and the resulting inter-electrode capacitance can change dramatically.

According to the potential boundary conditions of an MUT, planar capacitive sensors can be categorised into three different sensing modes:

- 1 the transmission mode for a floating MUT;
- 2 the shunt mode for a grounded MUT; and
- 3 the single-electrode mode with an MUT used as a virtual electrode in a capacitor.

To further explain the sensor response and design issues for different sensing modes, it is necessary to review the general aspects of sensor design issues and parameters for performance evaluation.

### Key issues for sensor design, performance evaluation and considerations for instrumentation

There are a number of issues in sensor design and several parameters for evaluating the performance of a sensor. One design issue may influence the sensor performance in several aspects. On the other hand, more than one design issues may have to be considered together to achieve the desired sensor performance. Therefore, it is important to understand how the design issues influence the sensor performance, so that a sensor can be optimised for a specific application. In addition, instrumentation-related issues need to be considered to obtain correct measurements from a sensor. The key issues in sensor design and construction, parameters for performance evaluation and instrumentation-related issues are briefly summarised in this section. The detailed discussions on sensor design and evaluation related issues can be found in sensor modelling and evaluation parts in this paper or from the references provided. Owing to the scale of this paper, the details of the instrumentation-related issues are not included here, but can be found in references provided.

#### Sensor design

The key design issues for a planar sensor include the number of electrodes and their arrangement, geometry of electrodes, shielding and guarding.

Number of electrodes and their arrangement depends on the number and complexity of the system variables to be solved for an application. It requires the understanding of the relationship between capacitance measurements and system variables. For a simple application, such as proximity or displacement measurement, where there exists a direct relationship between capacitance measurements and the distance of an MUT, a single sensing element, such as a concentric ring sensor, would be sufficient to infer the proximity of the MUT from capacitance measurement. For more complex situations, such as imaging or NDT-related applications, a sensor array may be used to provide a set of measurements for image

reconstruction or parameter estimation. The arrangement of electrodes in the sensor array may need to be considered. The arrangement of electrodes also depends on the available space in the system to place the electrodes.

Geometry of electrodes includes the shape, spacing and separation of electrodes, which are the most important parameters to determine the sensor performance (Li *et al.*, 2006). The shape of electrodes can be in a simple form, such as a square, rectangular, round or ring shape, or in a complex form, such as a comb or spiral shape. The spacing between electrodes refers to the distance between the centres of two adjacent electrodes. The separation of electrodes refers to the width of the empty space between the adjacent electrodes. The geometry of electrodes influences the sensor performance in signal strength, penetration depth and measurement sensitivity, as will be illustrated later in this paper.

Shielding and guarding can be used for shaping the electric field (Quantum Research Group, 2005), and more importantly for eliminating stray capacitance and noise from an unwanted region (Li *et al.*, 2006). Different types of shielding and guarding methods may be used, depending on the capacitance measuring circuit. Usually, a shield is held at a ground potential. Shielding can be placed in between the electrodes or beneath the substrate as a backplane (Li *et al.*, 2006). Active guarding is another commonly used method in capacitance measurement, where a guard electrode is held at the same potential as the driving signal (Huang *et al.*, 1988). Shielding and guarding should be considered together with instrumentation-related issues.

#### Sensor construction

An insulation layer is usually placed over the electrodes in a capacitance sensor to prevent the direct contact to an MUT. A sensor substrate is used as mechanical support. The issues in sensor construction include the choice of materials for the electrodes, insulation layer, substrate and the choice of a construction method. Electrodes are commonly made of a conductive material, such as copper. Dielectric materials are used to for the insulation layer and the sensor substrate. The choice of material would affect the sensor performance by introducing additional uncertainty or drift in capacitance measurements. It is desirable to use materials of low-moisture absorption, so that their influences to measurements are minimal (Mamichev *et al.*, 1998). The permittivity value for the sensor substrate and the insulation layer should be chosen to be as close to the value of the MUT as possible, so that the electric field in the system is the most uniform (Xie *et al.*, 1990). The thicknesses of the insulation layer and the sensor substrate can influence the signal strength and the sensitivity distribution, and thus need to be optimised (Li *et al.*, 2006). Several sensor construction techniques, including MEMS (Chen and Luo, 1998), printed circuit board (PCB) and manual construction, can be chosen, depending on the dimension of the sensor and costs.

#### Key parameters for evaluation of sensor performance

To evaluate the performance of a sensor, the parameters to be considered include signal strength, dynamic range, linearity, penetration depth, measurement sensitivity and cross-talk. For imaging applications, further evaluation parameters need to be considered, including spatial/image resolution, sensitivity distribution and imaging speed.

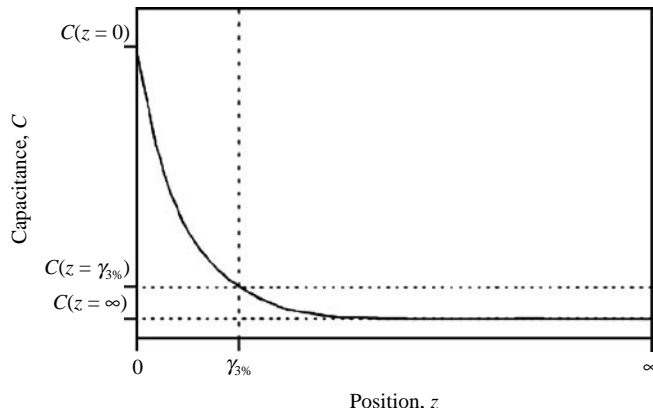
Signal strength and dynamic range the feature of a planar sensor is that the signal decreases exponentially in the  $z$ -direction (Mamishev *et al.*, 2004). The output signal of a sensor consists of a standing value and the dynamic changes due to the presence of an MUT. The standing value is the measurement from an empty sensor, which is often much larger than the dynamic range. For example, the standing capacitance is about one order larger than the changes in capacitance in an electrical capacitance tomography (ECT) sensor (Yang, 1996). One of the objectives in sensor design is to minimise the standing value and maximise the dynamic range, so that a maximum signal-to-noise ratio can be achieved.

Linearity due to the soft-field nature, the response of a capacitance sensor to material properties is inherently non-linear (Yang and Peng, 2003). However, for some applications, such as proximity or displacement measurement, there is an approximated linear region near the origin in capacitance measurement (Chen and Luo, 1998). The linear range and the slope of this approximated linear region determine the working range and the sensitivity of a capacitance-based proximity sensor.

The penetration depth for a planar sensor can be defined as maximum the distance in the  $z$ -direction for the sensor to produce a detectable change in the sensor output. It is an important parameter to indicate how far the sensor signal can reach. In literature, a threshold of 3 per cent of the dynamic range is used to define the  $z$  distance as the penetration depth when an MUT is moving away from the sensor electrodes (Figure 2(a)) (Li *et al.*, 2006). It is also desirable to study how deep the electric field can penetrate into an MUT. In the same way, the penetration depth against the thickness of an MUT can be defined, as shown in Figure 2(b) (Da Silva, 2008). In practice, the penetration depth is limited by the noise level of the instrumentation system, and is affected by the spacing between electrodes.

In general, sensitivity is defined as the ratio of changes in the sensor output to changes in a system variable. The linearised sensitivity (i.e. neglecting the second and higher order terms) for capacitance measurement can be written as (Yang and Peng, 2003):

$$\Delta C = s_\varepsilon \Delta \varepsilon \quad (4)$$



(a) C vs MUT lift-off

where  $s_\varepsilon = d\xi/d\varepsilon$  is the sensitivity of the capacitance transducer to changes in permittivity. One feature of capacitance sensors is that multiple system variables are coupled in the inter-electrode capacitance measurement, including permittivity ( $\varepsilon$ ), conductivity ( $\sigma$ ), lift-off ( $l$ ) and thickness ( $t$ ) of an MUT.

In NDT or imaging applications, sensitivity distribution can be obtained, and used to evaluate the sensor performance or used for image reconstruction. Among different methods for obtaining the sensitivity distribution (Wajman *et al.*, 2004), the numerical method based on the dot multiplication is a popular choice due to the advance in computing and numerical modelling techniques (Li, 2008). By modelling with high orders and using a fine mesh, a sensitivity distribution with high accuracy can be generated. Based on the superposition theory (Yang, 2007), a sensitivity distribution for a complex electrode arrangement can also be generated. The 3D sensitivity distribution for a pair of driving and sensing electrodes can be derived by Xie *et al.* (1990) and Wajman *et al.* (2004):

$$S_{SDj} = - \int_P \frac{E_{Dj}}{V_D} \cdot \frac{E_{Sj}}{V_S} dv_j \quad (5)$$

where  $E_{Dj}$  and  $E_{Sj}$  are the electric fields in a voxel  $j$  when potentials  $V_D$  on electrode D and  $V_S$  on electrode S are set and  $v_j$  is the volume of the  $j$ th voxel and  $P$  is the sensing space.

The sensitivity distribution can be evaluated by the sensitivity variation parameter (SVP), as defined by Xie *et al.* (1990):

$$SVP = \frac{S_{\varepsilon,dev}}{S_{\varepsilon,avg}} \quad (6)$$

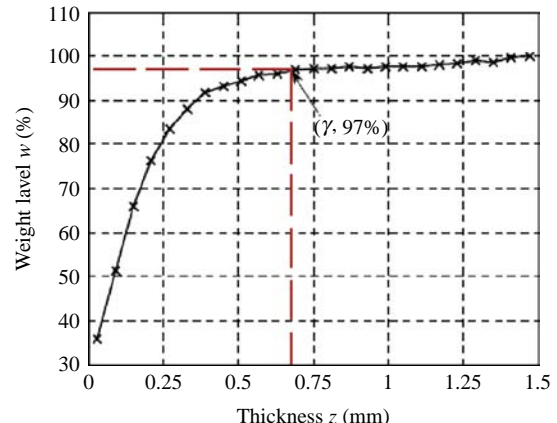
where:

$$S_{\varepsilon,avg} = \frac{1}{M} \sum_{j=1}^M S_{\varepsilon,j} \quad (7)$$

and:

$$S_{\varepsilon,dev} = \left( \frac{1}{M} \sum_{j=1}^M (S_{\varepsilon,j} - S_{\varepsilon,avg})^2 \right)^{1/2} \quad (8)$$

**Figure 2** Effective penetration depth of an FEF sensor against lift-off and thickness of MUT



(b) C vs MUT thickness

The smaller the SVP, the more homogeneous the sensitivity distribution is.

Cross-talk indicates the influence of a sensing element on its neighbouring elements, which should be kept minimal in practice. However, as a fringe field is dominant in planar sensors, unwanted coupling between different sensing elements is inevitable. Cross-talk can be reduced by using a shield (Li *et al.*, 2006) or by increasing the separation between the adjacent sensing elements, at the cost of weakened signal strength or a poorer spatial resolution.

Spatial resolution refers to the smallest feature that can be detected by a sensing element. It depends on the geometry of the electrodes and their arrangement. Image resolution refers to the size of pixels in an image. It depends not only on the spatial resolution of the sensor, but also on the image reconstruction algorithm. In some applications, a measurement from each sensing element is directly mapped into a pixel in an image, such as in fingerprint imaging (Lee *et al.*, 1999). In other applications, the sensitivity distribution is used to generate an image, where the number of pixels is larger than the number of measurements (Cheng, 2008).

Imaging speed depends on the data acquisition speed of a measurement system and the algorithm used for image reconstruction.

### Instrumentation-related issues

The instrumentation-related issues include measurement protocol, stray-immunity and capacitance measuring method.

Measurement protocol refers to the pattern and sequence for energising the driving electrodes and taking measurements from the sensing electrodes. A number of measurement protocols can be implemented with a sensor array, e.g. a single electrode or multiple electrodes can be used for either driving or sensing. Different measurement protocols can result in different sensor responses, acquisition time and different number of measurements. It can also result in redundant measurements due to symmetry in electrode arrangement. An optimal measurement protocol may be needed for a specific application.

Stray-immunity should be considered in a capacitance measuring circuit due to the existence of stray capacitance, which can be much larger than the sensor capacitance itself (Yang, 1996). Stray-immunity can be ensured by a stray-immune configuration or by using guard electrodes (Huang *et al.*, 1988) (Figure 3).

In a stray-immune circuit, a measuring electrode is held at virtual ground. The stray capacitance can be modelled as two capacitors,  $C_{s1}$  connected from the driving electrode to ground, and  $C_{s2}$  between the virtual ground and ground.

$C_{s1}$  will not affect the measurement because the current flowing through it does not contribute to the current to be measured. Also,  $C_{s2}$  will not affect the measurement because both its terminals are held at ground potential. All the signal paths and electrodes should be protected by grounded shielding. In addition, both terminals of the unknown capacitor  $C_x$  can be committed into the measuring circuit.

In the active guard method, the influence of stray capacitance,  $C_s$ , is eliminated by the active guard, which is driven at the same potential as the excitation signal. A high-speed unity-gain buffer should be used to drive the active guard. The signal paths and the unused electrodes should all be actively driven, so that unwanted capacitive coupling can be eliminated (Quantum Research Group, 2005). In addition, only one terminal from the unknown capacitor can be committed into the measuring circuit.

The commonly used capacitance measurement methods with the consideration of stray-immune configuration include:

- the charge-transfer-based techniques, e.g. charge/discharge circuit (Huang *et al.*, 1988);
- the auto-balancing-bridge-based techniques, e.g. impedance analysers (Agilent, 2008a) and an AC-based ECT system (Yang and York, 1999); and
- the current-injection techniques (Nerino *et al.*, 1997; Cypress Semiconductor, 2007).

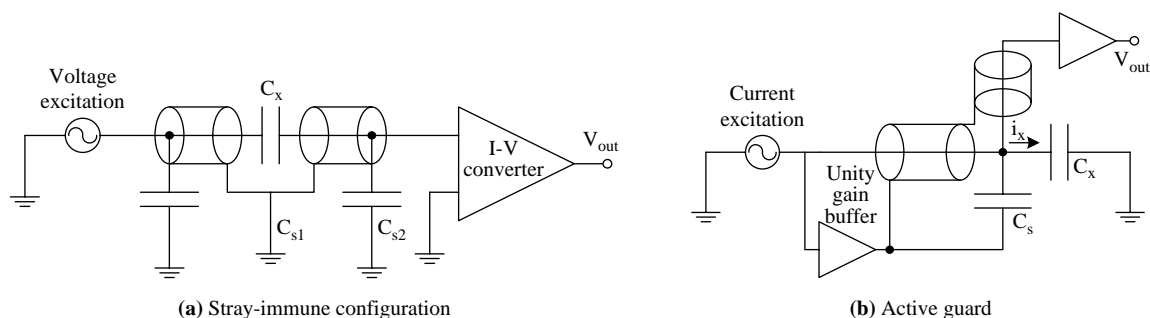
The charge/discharge and auto-balancing bridge techniques use a stray-immune configuration, and can be used with a planar capacitive sensor in the transmission or shunt mode. The current-injection techniques use the active guard method, and can be used with a planar capacitive sensor in the single-electrode mode.

### Sensor modelling, response and design guidelines

While analytical modelling can provide accurate solutions to sensors of simple geometries, numerical modelling is preferred to deal with varying design parameters and properties of an MUT. In this work, a commercial FEM package, COMSOL, is used for sensor modelling and simulations.

To understand the relationship between the design issues and the sensor performance, a concentric-ring-shaped capacitance sensor is used in modelling and simulations. This sensor is chosen because of its symmetry in structure, so that sensor modelling can be simplified. Simulations were carried out using COMSOL 3.4 with a 2D axial symmetric electro-statics generalised module to calculate the sensor output with varying design parameters (e.g. the radii of the

Figure 3 Stray-immune methods for capacitance measurement



driving electrode, the separation of electrodes, the width of the sensing electrode and the distance of the backplane to electrodes). The concentric ring sensor has an insulation layer of 0.5 mm thick, a sensor substrate of 5 mm thick and copper electrodes of 0.1 mm thick sandwiched in between. The material chosen for the insulation layer and sensor substrate is FR4, with a dielectric constant of 4.5 (Merkel *et al.*, 2000). The centre electrode is used for driving while the ring electrode is used for sensing. An MUT is placed in the upper half space ( $z \geq 0$ ). The backplane, if used, is on the bottom of substrate. To examine the sensor response in relationship with the material properties, positions and design parameters, capacitance measurements are plotted against the variable in evaluation.

### Transmission mode

In the transmission mode, an MUT is floating. Although the electrical properties of an MUT may change the distribution of the electric field in the system, the sensor can be modelled as a two-terminal system with three capacitors:

- 1 a capacitor between the driving and sensing electrodes,  $C_{ds}$ ;
- 2 a capacitor between the driving electrode and an MUT,  $C_{dm}$ ; and
- 3 a capacitor between the sensing electrode and an MUT,  $C_{sm}$ .

The sensor model, potential and field distributions, as well as an equivalent circuit for the planar capacitive sensor in the transmission mode are shown in Figure 4.

To investigate the sensor response to electrical properties of an MUT, simulations were carried out to find out the relationship between the inter-electrode capacitance and the permittivity or conductivity of the MUT. Figure 5 shows the absolute capacitance vs permittivity/conductivity. It can be seen that the inter-electrode capacitance increases with the increase in permittivity or conductivity, but the relationships are non-linear, due to the insulation layer used in the sensor. If the MUT is in direct contact with the sensor electrodes, the capacitance will be proportional to the permittivity (Da Silva, 2008).

To investigate the influence of the design parameters on the sensor performance, simulations were carried out to find out the relationship between the sensor output and different thicknesses and lift-off of an MUT. Figure 6 shows the capacitance measurement against a dielectric MUT with the consideration of varying design parameters.

In the transmission mode, the inter-electrode capacitance decreases with the lift-off of an MUT but increases with the thickness of an MUT. Using a bigger driving electrode or sensing electrode can increase the signal level, dynamic range and sensing depth. However, increasing electrode separation results in a reduced signal level and dynamic range but an enhanced penetration depth. This means that there is a trade-off in determining the electrode size and separation, and thus an optimal ratio between these parameters are needed to achieve the best overall performance. In addition, the penetration depth is roughly half of the electrode spacing. The use of backplane results in a reduced signal level, dynamic range and sensing depth. Therefore, it should be kept a certain distance away from the sensor electrodes. The use of inter-electrode shielding also reduces the signal level and dynamic range, but enhances the sensing depth and significantly extends the approximated linear region near the origin. To achieve an optimal design, the electrode spacing should be determined at first according to the desired penetration depth. The use of backplane and shielding may be considered, and an optimal ratio for electrode size and separation may be sought.

As the sensor output is directly related to the properties of an MUT, a planar capacitive sensor in the transmission mode is suitable for material characterisation, NDT, multi-interface sensing and tomography.

### Shunt mode

In the shunt mode, an MUT is grounded. It affects the capacitive coupling in the system by drawing electric field lines away from the sensing electrode, and thus, reduces the inter-electrode capacitance. The sensor can be modelled as a three-terminal system with three capacitors:

- 1 a capacitor between the driving and sensing electrodes,  $C_{ds}$ ;
- 2 a capacitor between the driving electrode and an MUT,  $C_{dm}$ ; and
- 3 a capacitor between the sensing electrode and an MUT,  $C_{sm}$ .

When an MUT is at a low potential instead of ground, such as a human body (Cheng, 2008), the sensor behaviour can be described by the shunt mode. The equivalent circuit in this case includes an additional capacitor between an MUT and ground,  $C_{mg}$ . The sensor model, potential and field distributions, and equivalent circuits for the planar capacitive sensor in the shunt mode are shown in Figure 7.

**Figure 4** Sensor model, potential and field distributions, and equivalent circuit for transmission mode

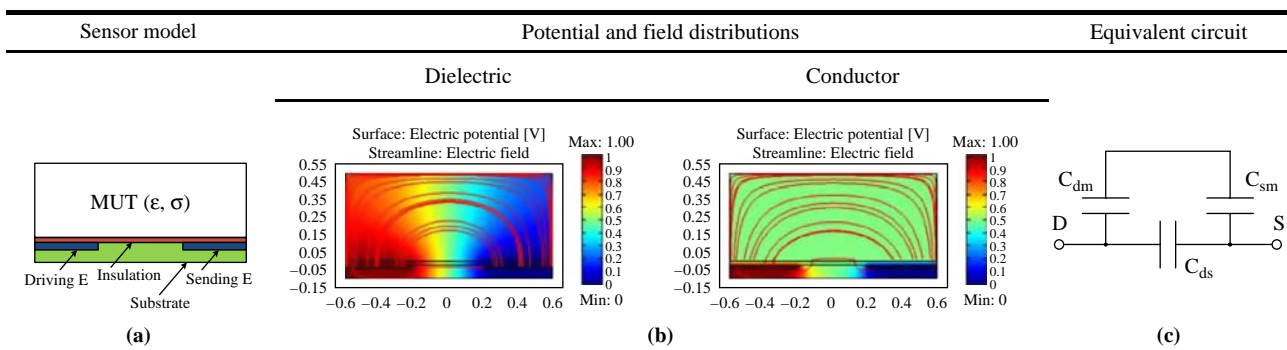
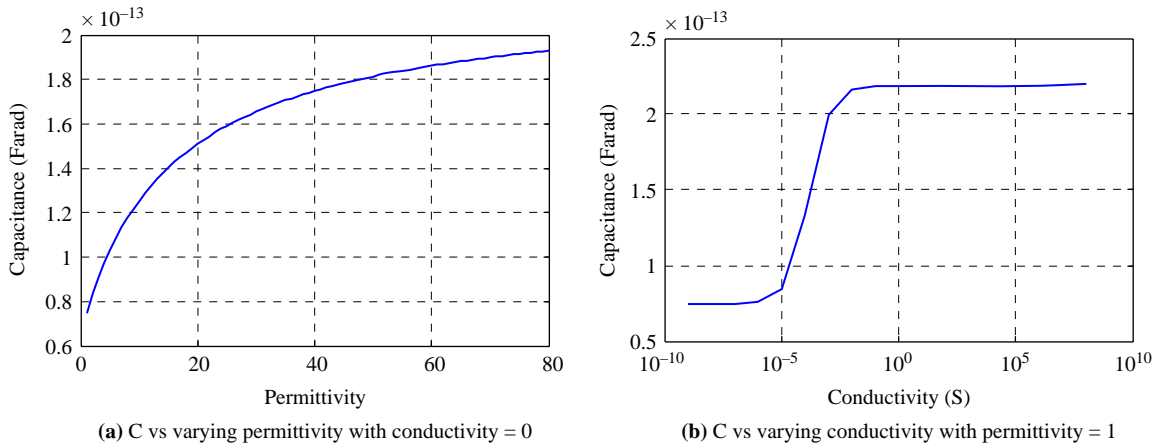


Figure 5 Capacitance measurements in response to properties of MUT from concentric ring sensor in transmission mode



Notes: Radii = 4 mm; ring width = 2 mm; separation = 2 mm; thickness of MUT = 11 mm; without backplane and inter-electrode shielding

Figure 6 Influence of design parameters on sensor response to dielectric MUT ( $\epsilon_r = 5$ ,  $\sigma = 0$ ) in transmission mode

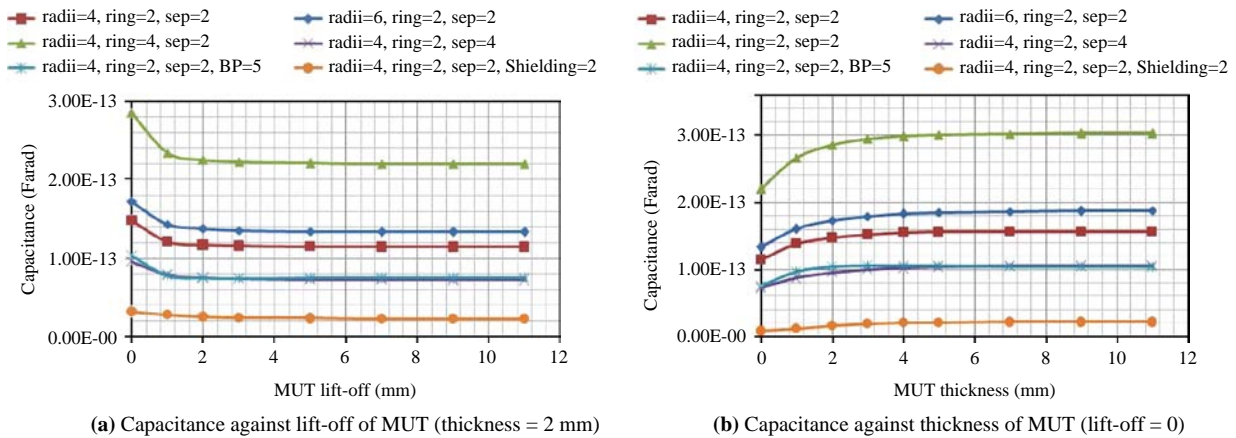
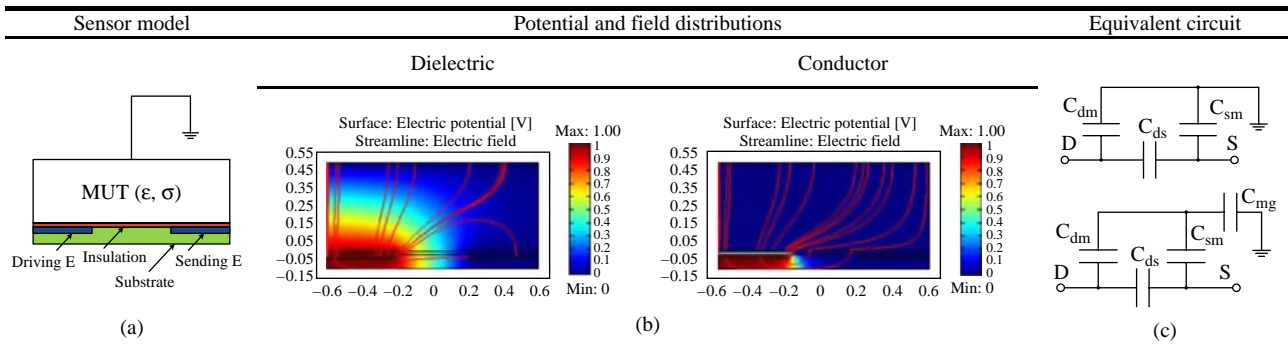


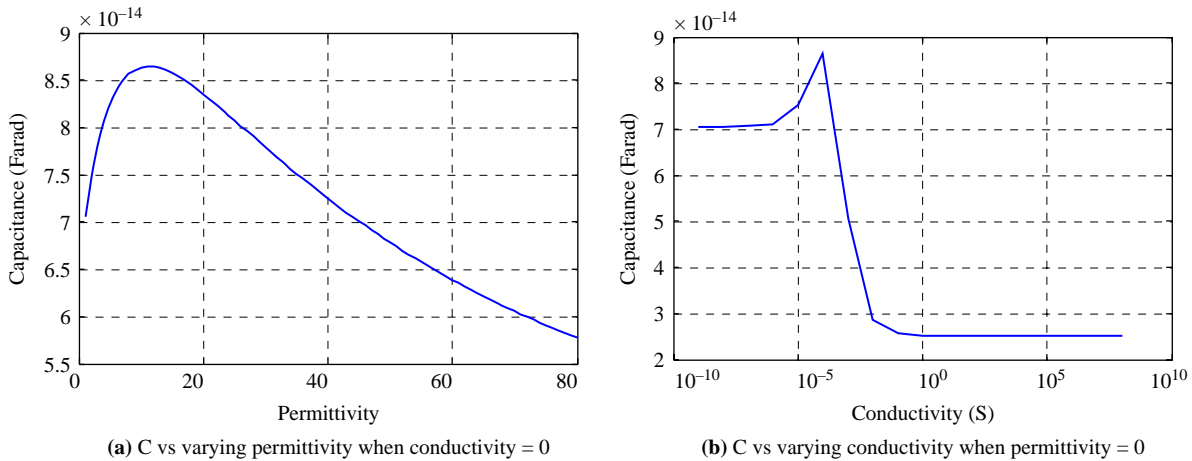
Figure 7 Sensor model, potential and field distributions, and equivalent circuit in shunt mode



To investigate sensor response to the properties of an MUT and design parameters, similar simulations were carried out. Figure 8 shows the absolute capacitance vs the permittivity and conductivity of an MUT. In the shunt mode, the inter-electrode capacitance increases non-linearly with the permittivity or conductivity of an MUT when the values are

low, but decreases sharply as their values continue to increase, because the higher the values of permittivity or conductivity, the more the field lines are drawn to the grounded boundary. It suggests that the sensor performance in the shunt mode is similar to the transmission mode when the permittivity/conductivity of an MUT is low, but different when the

**Figure 8** Capacitance measurements in response to properties of MUT from concentric ring sensor in shunt mode



**Notes:** Radii = 4 mm; ring width = 2 mm; separation = 2 mm; thickness of MUT = 11 mm; without backplane and inter-electrode shielding

permittivity/conductivity of an MUT is high. In addition, different permittivity or conductivity values could result in the same inter-electrode capacitance, which makes it more difficult to estimate the material properties.

Figure 9 shows capacitance measurements against a dielectric MUT with the consideration of varying design parameters.

Unlike in the transmission mode, the inter-electrode capacitance in the shunt mode increases both with the lift-off and thickness of an MUT. The influences of electrode geometry and shielding are similar to those on the transmission mode. However, the penetration depth in the shunt mode is larger than in the transmission mode, which is roughly 1.5 times of the electrode spacing, because the grounded MUT makes the electric field lines penetrate deeper into the MUT. In addition, the approximated linear region near the origin is much larger, especially with the use of inter-electrode shielding. The design guidelines for a planar capacitive sensor in the shunt mode are similar to those in the transmission mode.

As the inter-electrode capacitance is not directly related to the electrical properties of an MUT, it is difficult to use a

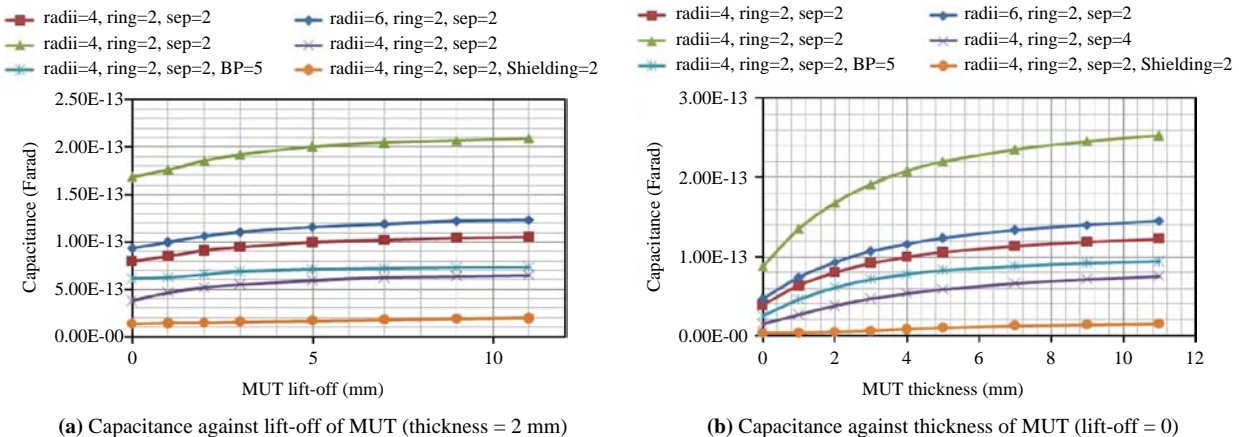
planar capacitive sensor in the shunt mode for material characterisation. On the other hand, the relevance of sensor output to the position of an MUT makes it suitable for displacement or proximity measurement.

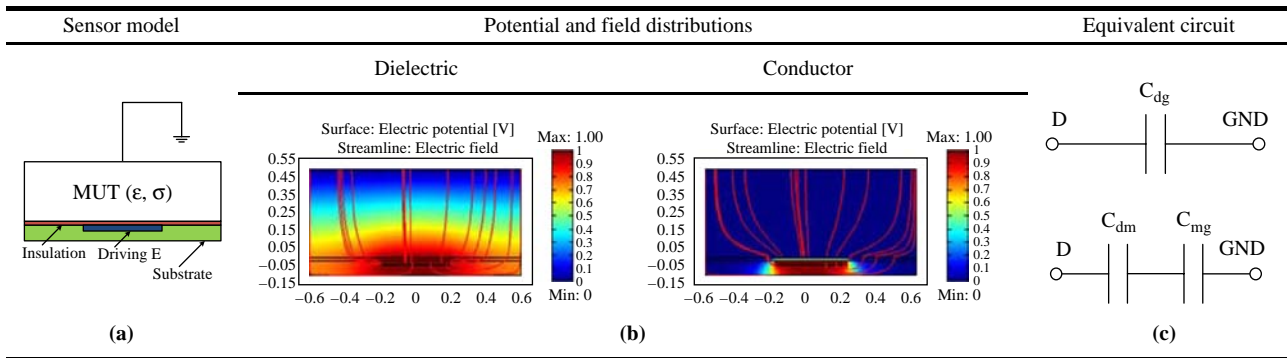
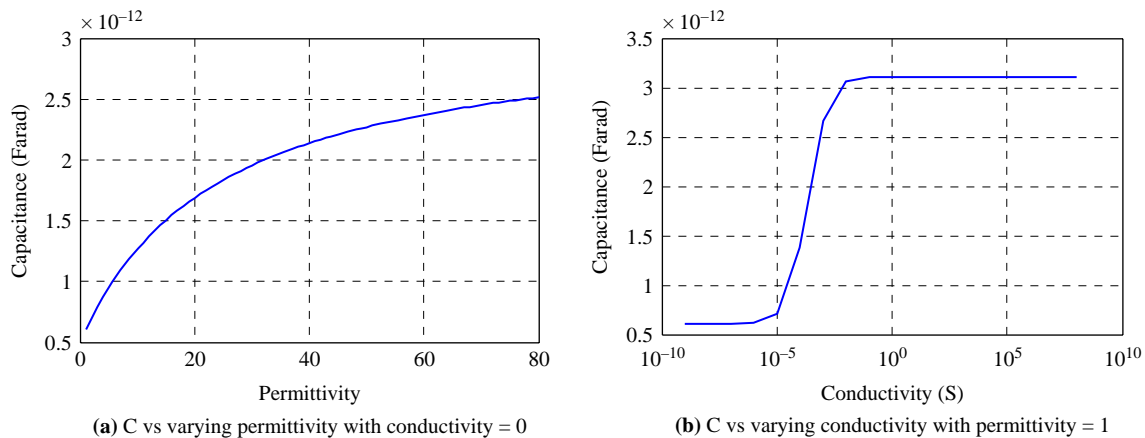
**Single-electrode mode**

In the single-electrode mode, an MUT is grounded, and is used as a virtual electrode. The electric field lines start from the driving electrode and terminate on the grounded boundary of the MUT. Therefore, the sensor can be modelled as a capacitor between the driving electrode and MUT,  $C_{dm}$ . When an MUT is at a low potential, the sensor behaviour can be described using the single electrode mode. The equivalent circuit in this case includes an additional capacitor between an MUT and ground,  $C_{mg}$ . The sensor model, potential and field distributions, and equivalent circuits for a planar capacitive sensor in the single-electrode mode are shown in Figure 10.

To investigate the sensor response to the properties of an MUT and the design parameters, similar simulations were carried out. Figure 11 shows the absolute capacitance against

**Figure 9** Influence of design parameters on sensor response to dielectric MUT ( $\epsilon_r = 5, \sigma = 0$ ) in shunt mode



**Figure 10** Sensor model, potential and field distributions, and equivalent circuit in single-electrode mode**Figure 11** Capacitance measurement in response to properties of MUT from concentric ring sensor in single-electrode mode

(a) C vs varying permittivity with conductivity = 0

(b) C vs varying conductivity with permittivity = 1

Notes: Radii for driving electrode = 4 mm; thickness of MUT = 5 mm

the permittivity and conductivity of an MUT. In the single-electrode mode, the measured capacitance increases non-linearly with the increase in the permittivity/conductivity of an MUT, which is similar to the transmission mode. However, the signal level is much larger because the capacitive coupling between the electrode and an MUT is stronger.

Figure 12 shows the capacitance measurements against the lift-off and thickness of a dielectric MUT with the consideration of varying radii and separation. Unlike in the transmission or shunt mode, the active guard technique should be used in the single-electrode mode, because an MUT cannot be connected into the measuring circuit. To avoid the unwanted coupling, the unused electrodes are connected to an active guard. Therefore, the design parameters include only radii and separation.

In the single-electrode mode, the inter-electrode capacitance decreases sharply with both the lift-off and thickness of an MUT. Using bigger electrodes can increase the signal level, dynamic range and penetration depth. Increasing the separation of electrodes also increases the signal level, dynamic range and penetration depth, because the active electrodes nearby will partly draw away the charge stored between the driving electrode and an MUT, and thus reducing the capacitance. The penetration depth is roughly 1 electrode spacing. To achieve an optimal design, the ratio between the electrode size and the separation needs to be considered.

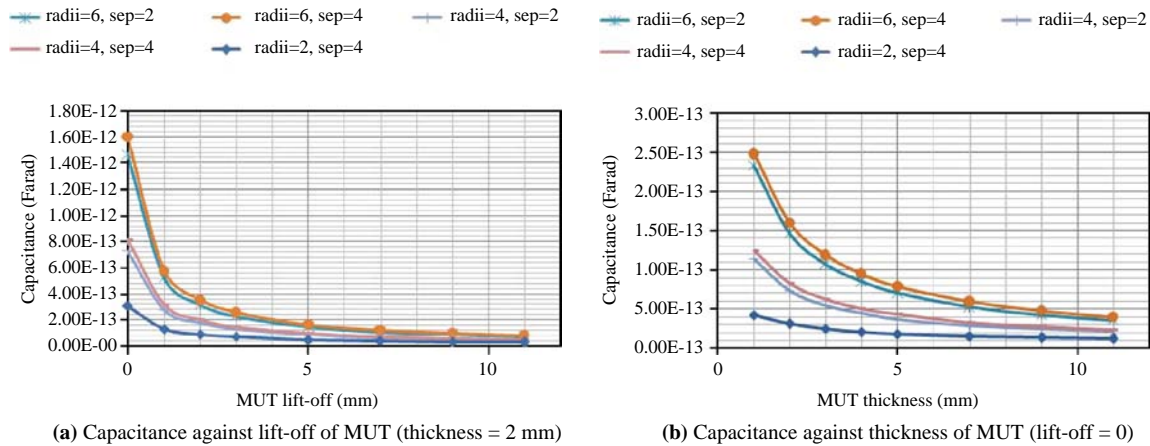
As the sensor output is directly related to the properties and positions of an MUT, a planar capacitive sensor in the single-electrode mode can be used for both material characterisation, imaging and proximity/displacement measurement.

### Sensitivity distributions

It is important to know the sensitivity distribution of a planar capacitance sensor. For non-imaging applications, the sensitivity distribution can be used to facilitate the sensor design and optimisation. For imaging applications, the sensitivity distribution is used for image reconstruction. The influence of the design parameters on the sensitivity distribution has not been studied for planar capacitive sensors so far. The influencing factors, such as electrode shape, separation and shielding, will be examined. SVP, as defined in the previous section, can be used to indicate how uniform the sensitivity distribution is, and how far the penetration depth is.

### Shape of electrodes

The sensitivity distributions for electrodes of different shapes have been investigated, including the square-spiral, comb, concentric ring and rectangular shapes in the transmission or shunt mode, and the square shape in the single-electrode mode. The same sensing space of  $20 \times 20 \times 20 \text{ mm}^3$  was used in

**Figure 12** Influence of design parameters on sensor response to dielectric MUT ( $\epsilon_r = 5$ ,  $\sigma = 0$ ) in single-electrode mode

simulation for each design, with electrodes placed in a plane  $z = 0$ , centred at  $(0, 0)$ , and a separation of 2 mm between electrodes. No backplane or shielding is used. Figure 13(a)-(e) shows the electrode geometries, sensitivity distributions in  $XY$  plane and cross-sectional plane, and SVPs.

It can be seen that the high-sensitivity values are mainly distributed along the gap between the electrodes, with higher values at sharp corners than at smooth electrode boundaries. A single-electrode sensor presents the most uniform sensitivity. Owing to the symmetry in structure, the concentric ring electrode has a sensitivity distribution symmetrical along its  $z$ -axis.

#### Separation of electrodes

To examine the influence of the separation of electrodes, the sensitivity distribution of the rectangular sensor with the doubled separation (4 mm) was derived. The electrode geometry, sensitivity distributions and SVP are shown in Figure 13(f). It can be seen that a wider separation results in a more uniform sensitivity distribution and a deeper penetration depth.

#### Backplane

To investigate the influence of backplane, the sensitivity distribution of the concentric ring sensor with a backplane placed at  $z = -2$  mm was derived. The electrode geometry, sensitivity distributions and SVP are shown in Figure 13(g). It can be seen that the use of backplane distorts the sensitivity distribution by pushing it to the other side. It also causes negative sensitivity values between the electrodes and the backplane, reduces penetration depth and makes the overall distribution less uniform.

#### Influence of buried conductor in dielectric MUT on capacitance measurement

It is well-known that a capacitance sensor is affected by conductivity. The influence of a conductor buried in a dielectric MUT on the performance of a planar capacitive sensor needs to be further studied for capacitive sensors working in different sensing modes. Simulations were carried out using a concentric ring capacitance sensor in different sensing modes. Capacitance measurements were calculated

for a conductor ( $\epsilon_r = 1$ ,  $\sigma = 1$ ) buried in a dielectric MUT ( $\epsilon_r = 5$ ,  $\sigma = 0$ ) at varying depths (0.5, 1, 2, 3, 4 mm), and then normalised against capacitance measurements without the conductor. Figure 14 shows the sensor models, the field and potential distributions and the normalised capacitance values against the buried depth.

It can be seen that the existence of the buried conductor causes a positive change in capacitance in the transmission and the single-electrode mode. However, the capacitance decreases non-linearly with the buried depth. In the shunt mode, the buried conductor causes a negative change in capacitance. However, the capacitance increases almost linearly with the buried depth.

The output from a planar capacitive sensor is a non-linear function of permittivity, conductivity and their distributions. With only capacitance measurement, it is difficult to distinguish the contributions of conductivity and permittivity if they both exist. To deal with this problem, an additional sensing modality can be introduced into the sensing system. For example, a dual-modality capacitive and magnetic sensor may be used to provide complementary measurements for an MUT.

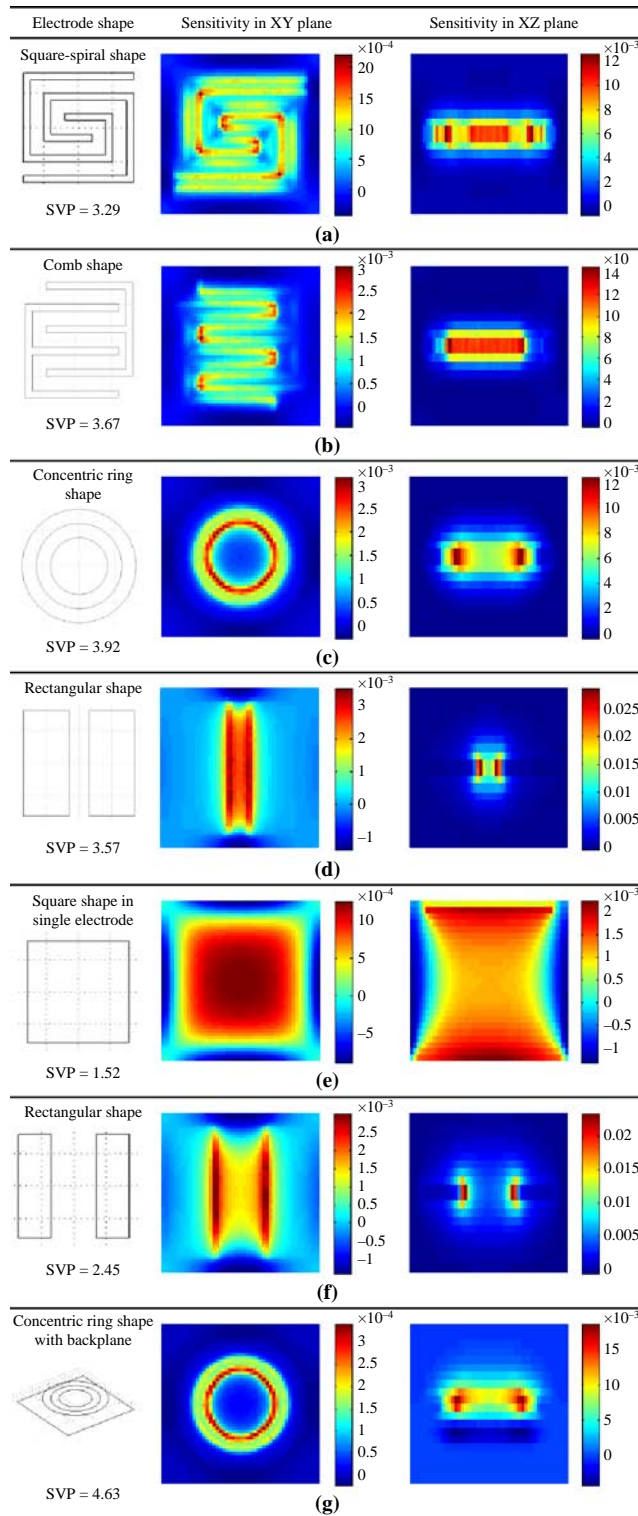
#### Applications

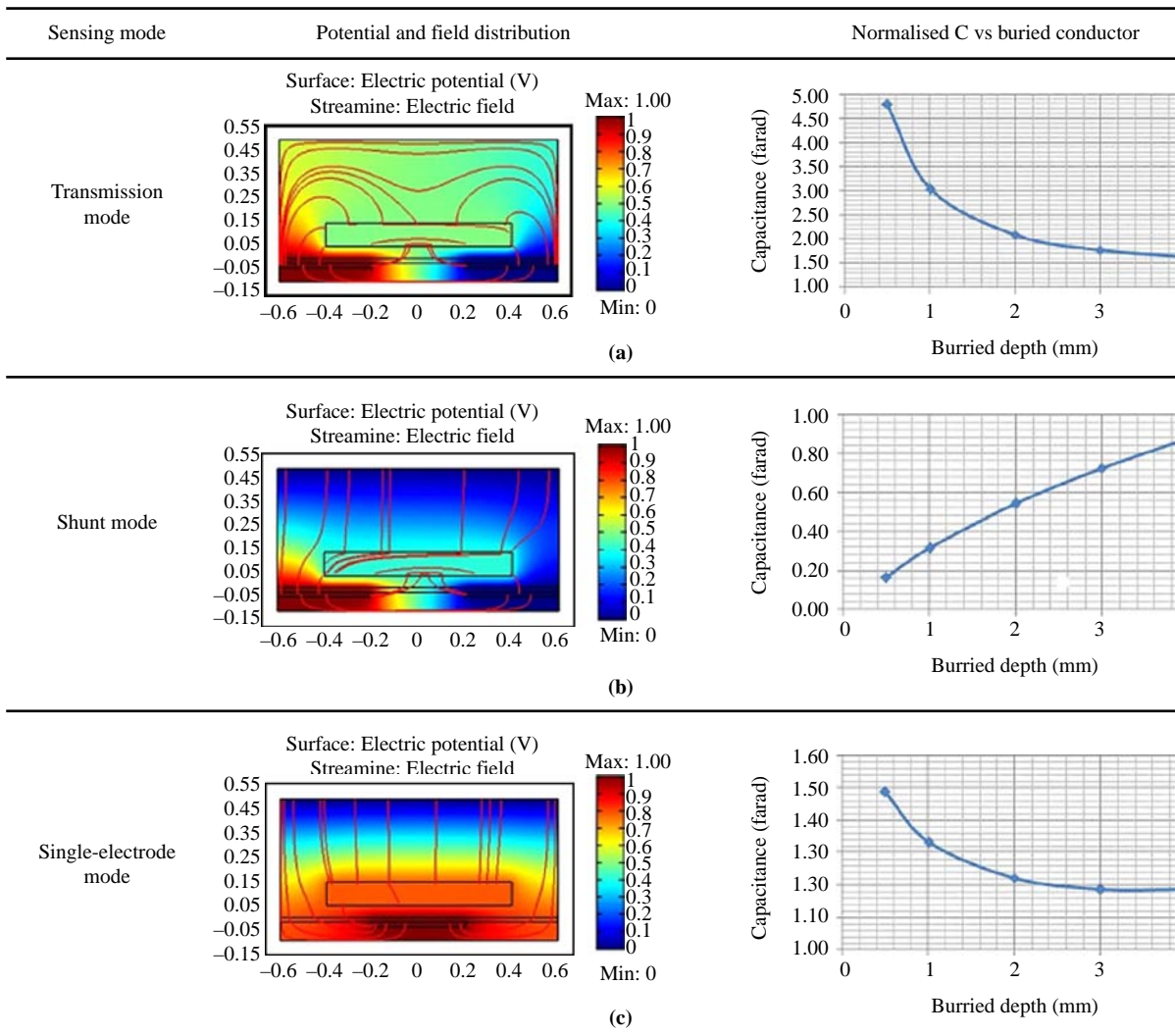
The applications of planar capacitive sensors can be categorised into non-imaging and imaging applications. For non-imaging applications, one or several system variables can be estimated based on the relationship between the sensor output and the system variable(s). For imaging applications, the estimated variables are presented as an image, which can be obtained from capacitance measurements by different image reconstruction methods, including direct imaging, model-based imaging and tomographic imaging.

In a direct imaging method, a direct mapping from a set of measurements to an image is sought, without solving the forward and inverse problems. An interpolation or statistical method may be used to increase the number of pixels or the image resolution. Applications based on the direct method include fingerprint imaging (Lee *et al.*, 1999) and inter-digital sensor-based flow imaging (Da Silva, 2008).

Model-based imaging makes use of a pre-computed sensor response from analytical models. The parameters of interest

Figure 13 Sensitivity distributions for electrodes with different shapes



**Figure 14** Influence of conductor in dielectric MUT in different sensing modes

are plotted into measurement grids or look-up tables. Inverse interpolation is used for estimation and imaging from measurements (Sheiretov, 2001). Although it is time-consuming to generate the measurement grid, the simplicity and fast speed of the inverse interpolation method makes it possible to implement parameter estimation and imaging online. Applications based on the model-based method include imaging with inter-digital sensors and sensor arrays (Schlicker, 2005; Schlicker *et al.*, 2006).

Tomographic imaging involves solving the forward problem to obtain the sensitivity distribution for a sensor, and solving the inverse problem to obtain an image (Xie *et al.*, 1990). In contrast to the model-based method, tomography has a relatively general applicability in that it can be used with different sensors and applications. In most electrical tomography applications, however, the inverse problem to be solved is often ill-posed and ill-conditioned (Yang *et al.*, 2003). To solve such a problem, either the non-iterative or iterative algorithm can be used. A non-iterative algorithm is relatively simple and can be implemented online. However, it can only achieve a moderate accuracy for qualitative analysis. If an image of higher accuracy is required, an iteratively

algorithm needs to be used, which can be time-consuming and difficult to implement on-line. Tomographic imaging has been used in dielectric imaging with ring-shaped capacitive sensor array (Frounchi and Dehkhoda, 2003), landmine detection and luggage scanning with square-electrode capacitive sensor array (Cheng, 2008).

Concluded from the review of applications, further research in imaging with capacitive sensor array is of interest, especially with the use of a planar capacitive sensor array in different sensing modes. In addition, combining different image reconstruction methods with the use of a sensor array can be considered.

In this paper, the designs of planar capacitive sensor arrays are presented as an application example, which is part of the ongoing research which investigates the detection of threat objects hidden in shoes, envelopes or small parcels by capacitive sensor arrays. The desired penetration depth for the capacitive sensor arrays is first considered. The most likely place to hide threat objects in a shoe is in its bottom layer. Amongst different types of shoes, leather shoes and trainers are of most interest, because they have a relatively thick and uniform bottom layer, which is about 1-2 cm thick.

Most envelopes and small parcels have a thickness less than 2 cm. Therefore, the desired penetration depth is about 1–2 cm. A spatial resolution in the order of 1 cm is desirable for the sensor arrays to be able to identify the shape features of a hidden object. To compromise the penetration depth and spatial resolution, the size of the sensing element for all the sensor arrays to be designed is chosen to be  $2 \times 2 \text{ cm}^2$ . Two types of capacitive sensor arrays are to be used – a concentric-ring-element-based sensor array which works in the transmission or the shunt mode, and a square-electrode-based sensor array which works in the single-electrode mode.

### Concentric-ring-element-based capacitive sensor arrays

With the given elementary size, the optimal design for the concentric ring-sensing element is a trade-off between the dynamic range and SVP of the sensor, which are determined by the combination of radii, ring width and separation of electrodes. To find out the optimal ratio between them, simulations have been carried out to compare the dynamic range and SVP of the sensor against varying design parameters in the transmission mode. A radius of 3, 4 and 5 mm for the centre electrode and a width of 1, 2 and 3 mm for the ring electrode are used in evaluation. To make full use of the sensing area, the separation between the adjacent sensing elements is chosen to be 2 mm, and the separation between the driving and sensing electrodes is chosen to be as large as possible. As the spacing of the sensing element is fixed, the penetration depth of the ring sensor is almost fixed. The dynamic range is given as the difference between the sensor output with a dielectric MUT ( $\epsilon_r = 5$ ,  $\sigma = 0$ , thickness = 10 mm) and the output of an empty sensor. Table I gives a comparison of the absolute dynamic ranges and SVPs for different designs. The optimal design should have a big dynamic range and a least SVP.

From the above results, it can be seen that the optimal set of parameters is: radii = 4 mm, width of ring = 2 mm. Therefore, the separation between the centre and the ring electrode is 3 mm and the separation between adjacent sensing elements is 2 mm. The ring sensor array can work in the transmission mode for scanning envelopes or small parcels, or work in the shunt mode for scanning shoes. The expected penetration depth for transmission mode is half of electrode spacing, which is about 4 mm. The expected penetration depth for the shunt mode is 1.5 times of electrode spacing, which is about 12 mm.

Ideally, a sensor array can be formed using any number of ring elements placed in rows and columns. The number of elements depends on the size of the target MUT. In the current design, two arrays of  $8 \times 12$  elements (equivalent to a sensing area of  $16 \times 24 \text{ cm}^2$ ) are used for scanning shoes – one for the left shoe and the other for the right shoe, while an array of  $6 \times 6$  (equivalent to a sensing area of  $12 \times 12 \text{ cm}^2$ ) elements is used

for scanning envelope or small parcels. The driving electrodes in the sensor array are connected in rows while the sensing electrodes are connected in columns, so that a fast scan can be achieved by a row-excitation and column-detection method. The ring sensor arrays have been manufactured using PCB and a piece of rubber sheet (1 mm thick) is adhered to the surface of the electrodes as an insulation layer.

Sensing depth against lift-off and thickness of MUT were examined for the ring sensor array in the transmission mode and the shunt mode. The capacitance measurements from the sensor arrays were taken by an impedance-analyser-based multi-channel system, which uses a specifically designed multiplier box to extend the number of measurement channels (Hu *et al.*, 2008). To make the ring sensor work in the shunt mode, a grounded top boundary needs to be used. To achieve this, a plastic cover (1 mm in thickness) adhered with grounded copper sheet (0.01 mm in thickness) can be used. The ring sensor array works in the transmission mode without using this grounded plastic cover, but in the shunt mode when the grounded cover is placed above the sensor array with a certain height. This plastic cover is also used for single-electrode array, which will be explained later.

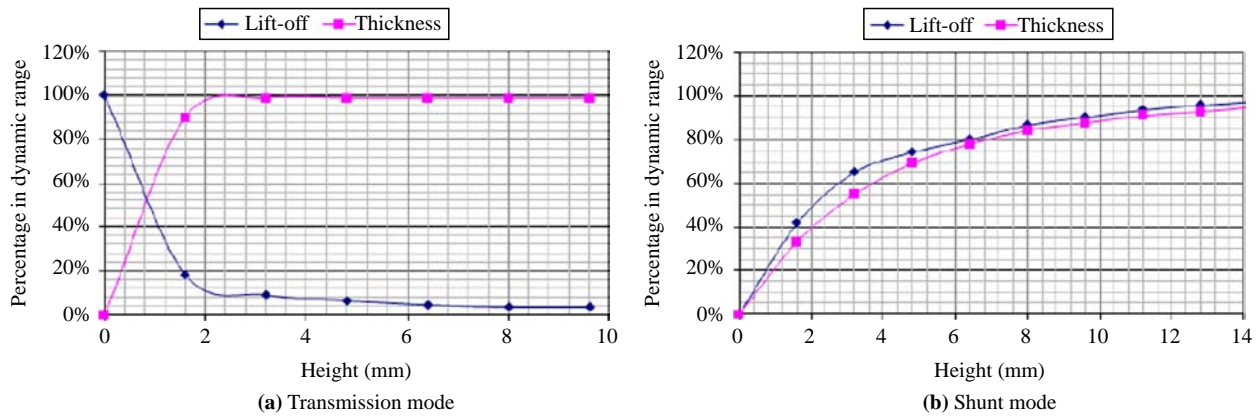
To examine the sensor response to lift-off of MUT, a square piece of Blu-Tack was placed at different heights above the same sensing elements, and the changes in capacitance against the dynamic range are shown in Figure 15(a). To examine the sensor response to thickness of MUT, square pieces of Blu-Tack with the same thicknesses were stacked over the same sensing element, and the changes in capacitance against the dynamic range are shown in Figure 15(b). The sensing depths for both cases are identified using the system noise level. For the optimal ring sensor in the transmission mode, the sensing depth is about 6 mm with a dynamic range of 109 fF against lift-off of MUT, and about 3 mm with a dynamic range of 554 fF against thickness of MUT. For the ring sensor in the shunt mode, the sensing depth is about 11 mm with a dynamic range of 273 fF against lift-off of MUT, and about 14 mm with a dynamic range of 651 fF against thickness of MUT. The order of the sensing depths is in agreement with simulations, but the dynamic range is much larger.

### Single-square-electrode capacitive sensor array

With the given elementary size, the optimal electrode size and separation can be found to compromise the dynamic range and cross-talk. For the single-electrode sensor array, the effective sensing region for one electrode may extend further beyond its boundaries due to the fringe field effect. This effective region can be quantified as sensing width, which can then be used to evaluate cross-talk for a single-electrode sensor. In this paper, the cross-talk for the single-electrode sensor is defined as the ratio between the sensing width and the spacing of electrodes:

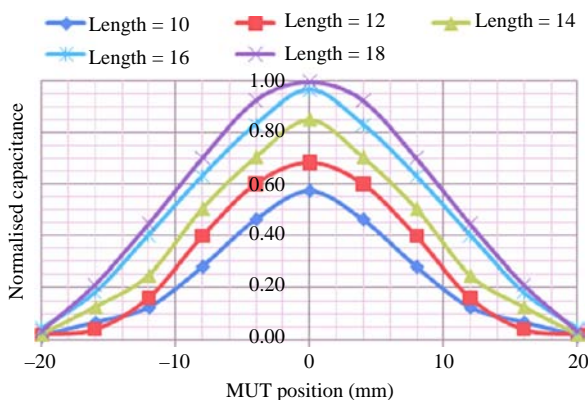
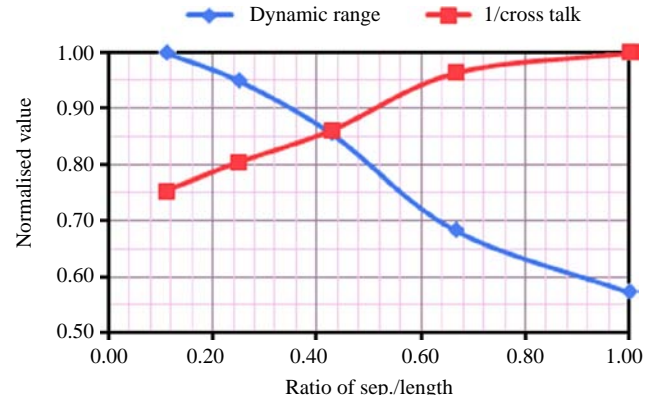
Table I Dynamic range and SVPs for different designs

Radii (mm)	3		4		5	
	Dynamic range (fF)	SVP	Dynamic range (fF)	SVP	Dynamic range (fF)	SVP
1	13.6	2.80	16.3	2.72	20.7	2.93
2	30.6	3.10	37.3	3.11	48.9	3.60
3	50.9	3.68	63.1	3.91	83.1	5.60

**Figure 15** Sensing depth for ring-shaped capacitive sensor in transmission mode and shunt mode

$$\text{Crosstalk} = \frac{\text{Sensing width}}{\text{Spacing of electrodes}} \quad (9)$$

Sensing width of the single-electrode sensor is investigated at first. A single-electrode sensor is modelled by COMSOL using a 3D electro-static generalised module. The sensing space is  $60 \times 60 \times 20 \text{ mm}^3$ . The top boundary of the sensing space is set to ground and all the other outer boundaries set to electric insulation. The electrode has a varying side-length of 10, 12, 14, 16 and 18 mm, which corresponds to electrode separation of 10, 8, 6, 4 and 2 mm. A small dielectric MUT ( $10 \times 10 \times 10 \text{ mm}^3$ ,  $\epsilon_r = 5$ ,  $\sigma = 0$ ) is moved along the  $X$ -axes, and the normalised capacitance for different electrode sizes are plotted against the position of the MUT, as shown in Figure 16. It can be seen that the normalised value at the boundary of the sensing element is well above 0. However, the effective sensing width can be determined using a threshold of 20 per cent of the dynamic range (Da Silva, 2008). Owing to symmetry, the sensing width in the  $Y$ -direction is assumed to be the same. The optimal single-electrode sensor should have a large dynamic range and a small cross-talk. Figure 17 shows the normalised dynamic range and  $1/\text{cross-talk}$  against the ratio of separation and length of electrodes. An optimal ratio of 0.43 is found at the cross point, which leads to a side-length of 14 mm for the electrode and a separation of 6 mm. A single-electrode array with  $6 \times 6$  square electrodes has been manufactured using PCB and a rubber sheet (1 mm thick) is adhered to the surface of the electrodes as the insulation layer.

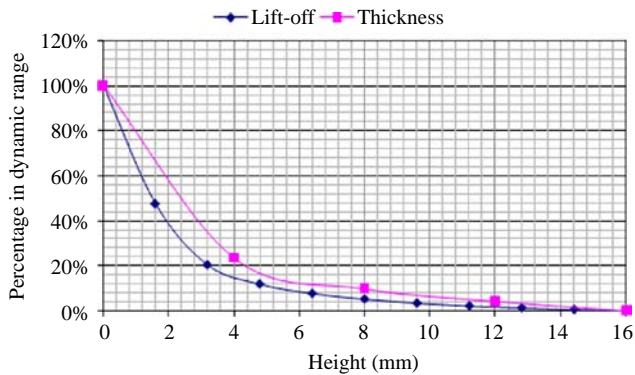
**Figure 16** Normalised capacitance against position of MUT**Figure 17** Normalised dynamic range and  $1/\text{cross-talk}$  against ratio of separation/length

Sensing depths against lift-off and thickness of MUT for the single-electrode sensor were evaluated, with the capacitance measurements also taken by the impedance-analyser-based multi-channel system. A plastic cover with two copper sheets was used together with the sensor board. The bottom copper sheet was used as a big virtual electrode, and the top copper sheet was used as grounded shield. To examine the sensor response to life-off of MUT, a square piece of Blu-Tack was placed at different heights above the same sensing elements. To examine sensor response to thickness of MUT, square pieces of Blu-Tack with the same thicknesses were stacked over the same sensing element. In both cases, the grounded virtual electrode was placed right above the test sample. The changes in capacitance against the dynamic range for lift-off and thickness of MUT are shown in Figure 18.

Using the noise level of capacitance measurement, the sensing depth can be identified. For the single-electrode sensor, the sensing depth is about 10 mm with a dynamic range of 4.53 pF against lift-off of MUT, and about 12 mm with a dynamic range of 4.13 pF against thickness of MUT. The order of the sensing depths is in agreement with simulations, but the dynamic range is much larger.

The influence of conductivity on the performance of planar capacitive sensors in different sensing modes was experimentally evaluated. A square piece of copper sheet

**Figure 18** Sensing depth against lift-off and thickness for capacitive sensor in single-electrode mode



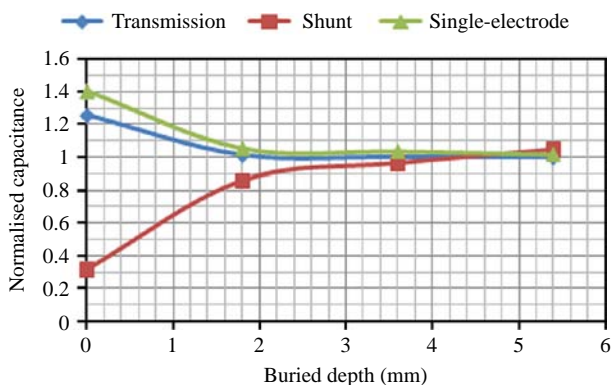
(0.1 mm thick,  $2 \times 2 \text{ cm}^2$ ) was inserted at different depth between several square pieces of Blu-tack used previously. The capacitance measurements in response to copper sheet buried at different depths were normalised against the measurement without copper sheet, and are plotted against the buried depth as shown in Figure 19. It can be seen that the copper sheet causes positive changes in capacitance for capacitive sensors in the transmission mode and the single-electrode mode, but causes negative changes in the shunt mode, which is in agreement with the simulations. However, the relationships between the normalised capacitance and the buried depth are not linear for all cases.

The designs of the different planar capacitive sensor arrays illustrate how to utilise sensor modelling methods to facilitate sensor design for a specific application. In addition, the experimental results confirm the usefulness of simulations in predicting the sensing depths for the capacitive sensor arrays. The influence of buried conductor on capacitance measurements has also been evaluated experimentally, with the results in agreement with simulations. Future research includes image reconstruction with different planar capacitive sensor arrays and evaluation of imaging results.

## Conclusions

In this paper, the sensing mechanism and the key issues in sensor design and performance evaluation have been discussed.

**Figure 19** Normalised capacitance vs buried copper in Blu-Tack for planar capacitive sensors in different sensing modes



According to the potential boundary conditions of an MUT, a planar capacitance sensor can be described by one of the three different sensing modes:

- 1 the transmission mode;
- 2 the shunt mode; and
- 3 the single-electrode mode.

The sensor response to the properties and positions of an MUT has been discussed in detail. To achieve an optimal design, a trade-off between different parameters has to be made. In the transmission mode and the single-electrode mode, the sensor response is strongly related to the properties of an MUT, which makes the sensor suitable for material characterisation and imaging. In the shunt mode, the sensor response is strongly related to the positions of an MUT, and hence the sensor is suitable for proximity/displacement measurement. The sensitivity distribution of a sensor depends largely on the geometry of the electrodes. In addition, the effect of conductivity on the sensor performance has been investigated, showing that it causes positive changes for a sensor in the transmission and single-electrode mode, but negative changes in the shunt mode.

An application example has been presented to illustrate how to utilise the sensor modelling methods to facilitate the sensor design. To detect threat objects hidden in shoes, envelopes or small parcels, different planar capacitive sensor arrays have been designed and manufactured using PCB, including the capacitive sensor arrays with concentric-ring elements, which work in the transmission mode or the shunt mode, and the capacitive sensor array with square electrodes, which works in the single-electrode mode. The experimental results show that the sensing depths of the sensor arrays and the influence of buried conductor on capacitance measurements are in agreement with simulations. Future research includes image reconstruction with different planar capacitive sensor arrays and evaluation of imaging results.

## References

- Agilent (2008a), *Data Sheet for Agilent 4294 Precision Impedance Analyser*, available at: [www.home.agilent.com/agilent/product.jsp?pn=4294A&NEWCCCL=USeng](http://www.home.agilent.com/agilent/product.jsp?pn=4294A&NEWCCCL=USeng)
- Agilent (2008b), "New technologies for accurate impedance measurement (40 Hz to 110 MHz)", Produce note 4294A, available at: <http://cp.literature.agilent.com/litweb/pdf/5968-4506E.pdf>
- Chen, Z.C. and Luo, R.C. (1998), "Design and implementation of capacitive proximity sensor using microelectromechanical systems technology", *IEEE Trans. Ind. Electron.*, Vol. 45, pp. 886-94.
- Cheng, B. (2008), "Security imaging devices with planar capacitance sensor arrays", PhD thesis, The University of Manchester, Manchester.
- COMSOL (2008), *AC/DC Module User Guide*, COMSOL, Burlington, MA.
- Cypress Semiconductor (2007), "Capacitive sensing techniques and considerations", available at: [www.cypress.com/?rID=3569](http://www.cypress.com/?rID=3569)
- Da Silva, M. (2008), "Impedance sensors for fast multiphase flow measurement and imaging", PhD thesis, Technical University of Dresden, Dresden.
- Diamond, G.G. and Hutchins, D.A. (2006), "A new capacitive imaging technique for NDT", *European*

- Conference on NDT, 25-29 September, Berlin, poster 229, pp. 1-8.
- Frounchi, J. and Dehkhoda, F. (2003), “High-speed capacitance scanner”, *Proceedings of the 3rd World Congress on Industrial Process Tomography, Banff, 2-5 September*, pp. 846-52.
- Hu, X.H., Yang, M., Li, Y., Yang, W.Q. and de Lara, M. (2008), “An impedance-analyser-based multi-channel imaging system and its applications”, *IEEE International Workshop on Imaging Systems and Techniques, Chania, 10-12 September*, pp. 181-6.
- Huang, S.M., Plaskowski, A.B., Xie, C.G. and Beck, M.S. (1989), “Tomographic imaging of two-component flow using capacitance sensors”, *J. Phys. E: Sci. Instrum.*, Vol. 22, pp. 173-7.
- Huang, S.M., Stott, A.L., Green, R.G. and Beck, M.S. (1988), “Electronic transducers for industrial measurement of low value capacitances”, *J. Phys. E: Sci. Instrum.*, Vol. 21, pp. 242-50.
- Igreja, R. and Dias, C.J. (2004), “Analytical evaluation of the interdigital electrodes capacitance for a multi-layered structure”, *Sens. and Actuators A: Phys.*, Vol. 112, pp. 291-301.
- Lee, J.W., Min, D.J., Kim, J. and Kim, W. (1999), “A 600-dpi capacitive fingerprint sensor chip and image-synthesis technique”, *IEEE J. of Solid-State Circuits*, Vol. 34, pp. 469-75.
- Li, X.B., Larson, S.D., Zyuzin, A.S. and Mamishev, A.V. (2006), “Design principles for multichannel fringing electric field sensors”, *IEEE Sensors J.*, Vol. 6, pp. 434-40.
- Li, Y. (2008), “Key issues of 2D/3D image reconstruction in electrical tomography”, PhD thesis, The University of Manchester, Manchester.
- Mamichev, A.V., Lesieutre, B.C. and Zahn, M. (1998), “Optimisation of multi-wavelength interdigital dielectrometry instrumentation and algorithms”, *IEEE Trans. on Dielectrics and Electric Insulation*, Vol. 5 No. 3, pp. 408-20.
- Mamishev, A.V., Sundara-Rajan, K., Yang, F., Du, Y. and Zahn, M. (2004), “Interdigital sensors and transducers”, *Proceedings of the IEEE*, Vol. 92, pp. 808-45.
- Merkel, T., Pagel, L. and Glock, H.W. (2000), “Electric fields in fluidic channels and sensor applications with capacitance”, *Sens. and Actuators A: Phys.*, Vol. 80, pp. 1-7.
- Nerino, R., Sosso, A. and Picotto, G.B. (1997), “A novel AC current source for capacitance-based displacement measurement”, *IEEE Trans. Instrum. Meas.*, Vol. 46 No. 2, pp. 640-3.
- Quantum Research Group (2005), “Secrets of a successful QTouch™ design”, Quantum Research Application Note AN-KD02, Rev. 1.03, Quantum Research Group, Southampton, October.
- Schlicker, D. (2005), “Imaging of absolute electrical properties using electroquasistatic and magnetoquasistatic sensor arrays”, PhD thesis, Massachusetts Institute of Technology, Cambridge, MA.
- Schlicker, D., Washabaugh, A., Shay, I. and Goldfine, N. (2006), “Inductive and capacitive array imaging of buried objects”, *Insight-Non-Destructive Testing and Condition Monitoring*, Vol. 48, pp. 302-6.
- Sheiretov, Y. (2001), “Deep penetration magnetoquasistatic sensors”, PhD thesis, Massachusetts Institute of Technology, Cambridge, MA.
- Shi, T.M., Xie, C.G., Huang, S.M., Williams, R.A. and Beck, M.S. (1991), “Capacitance-based instrumentation for multi-interface level measurement”, *Meas. Sci. Technol.*, Vol. 2, pp. 923-33.
- Smith, J., White, T., Dodge, C., Paradiso, J. and Gershenfeld, N. (1998), “Electric field sensing for graphical interfaces”, *IEEE Computer Graphics and Applications*, Vol. 18 No. 3, pp. 54-60.
- Wajman, R., Mazurkiewicz, L. and Sankowski, D. (2004), “The sensitivity map in the image reconstruction process for electrical capacitance tomography”, *Proceedings of the 3rd International Symposium on Process Tomography in Poland, Łódź, Poland, 9-10 September*, pp. 165-8.
- Wang, H.X., Yin, W.L., Yang, W.Q. and Beck, M.S. (1996), “Optimum design of segmented capacitance sensing array for multi-phase interface measurement”, *Meas. Sci. Technol.*, Vol. 2, pp. 79-86.
- Xie, C.G., Stott, A.L., Plaskowski, A. and Beck, M.S. (1990), “Design of capacitance electrodes for concentration measurement of two-phase flow”, *Meas. Sci. Technol.*, Vol. 1, pp. 65-78.
- Yang, M. (2007), “Development of electrical tomography systems and application for milk flow metering”, PhD thesis, The University of Manchester, Manchester.
- Yang, W.Q. (1996), “Hardware design of electrical capacitance tomography systems”, *Meas. Sci. Technol.*, Vol. 7, pp. 225-32.
- Yang, W.Q. and Peng, L.H. (2003), “Image reconstruction algorithms for electrical capacitance tomography”, *Meas. Sci. Technol.*, Vol. 14, pp. R1-R13.
- Yang, W.Q. and York, T.A. (1999), “New AC-based capacitance tomography system”, *IEE Proc.-Sci. Meas. Technol.*, Vol. 146 No. 1, pp. 47-53.
- Zeothout, J., Boletis, A. and Bleuler, H. (2003), “High performance capacitive position sensing device for compact active magnetic bearing spindles”, *JSM Int. J. Ser. B, Fluids and Thermal Eng.*, Vol. 46 No. 3, pp. 900-7.

### Further reading

- Metois, E., Yarin, P.M., Salzman, N. and Smith, J.R. (2002), “Fiber fingerprint identification”, *Proceedings of the 3rd Workshop on Automatic Identification, Tarrytown, NY, 14-15 March*, pp. 147-54.
- York, T.A., Evans, I.G., Pokusevski, Z. and Dyakowski, T. (2001), “Particle detection using an integrated capacitance sensor”, *Sens. and Actuators A: Phys.*, Vol. 92, pp. 74-9.

### Corresponding author

Xiaohui Hu can be contacted at: [huxiaohui1981@gmail.com](mailto:huxiaohui1981@gmail.com)